Constrained Motion Planning for Multiple Vehicles on SE(3)

Alessandro Saccon, A. Pedro Aguiar, Andreas J. Häusler, John Hauser, António M. Pascoal

***Abstract*— This paper proposes a computational method to solve constrained cooperative motion planning problems for multiple vehicles undergoing translational and rotational motions. The problem is solved by means of the Lie group projection operator approach, a recently developed optimization strategy for solving continuous-time optimal control problems on Lie groups. State constraints (for collision avoidance) are handled by means of a set of barrier functions, turning the optimization approach into an interior point method. A sample computation is shown to demonstrate the effectiveness of the method.**

I. Introduction

This papers addresses the problem of constrained cooperative motion planning for multiple vehicles undergoing translational and rotational motions that are naturally described in SE(3). The practical motivation for this study stems from a number of envisioned mission scenarios for autonomous underwater vehicles (AUVs). A representative example is when a number of AUVs equipped with acoustic and vision sensor units must cooperate to obtain marine habitat maps in complex 3D terrain that includes flat-like surfaces, near vertical cliffs, and overhangs. In this situation, it is crucial that the vehicles carrying distinct but complementary resources move together at close range and change their spatial formation according to the orientation of the terrain being mapped. This entails the development of a motion planner to solve the problem of generating reference trajectories that the vehicles should track in order to move from initial to target poses (positions and attitudes) in a coordinated manner. Such a planner must, at the final stage, include a reasonably accurate model of each vehicle and a possibly rough description of known terrain obstacles

The constraints that must be taken into consideration are twofold. The first is imposed by the fact that the vehicles must not collide with each other or with the environment. The second arises naturally from the fact that in order to do formation control the vehicles must use acoustic ranging devices and (at very close range) vision sensors to measure relative distances and attitudes. To avoid masking effects, it is crucial that nontrivial geometric constraints be imposed on the allowable motions.

Given the nature of the motion planning problem at hand, namely the presence of nontrivial geometric constraints and the need to take explicitly vehicle dynamics, actuator limitations, and (safety-related) state constraints into account, it is unlikely that standard path planning techniques can be applied to compute energy efficient maneuvers. We therefore exploit the use of a numerical optimal control approach that will allow for the introduction of nontrivial state and input constraints. At this stage, however, we restrict ourselves to kinematic models of the vehicles and take into account only inter-vehicle constraints.

The motion planner that we describe is based on the Lie group projection operator approach introduced in [1], [2]. This approach lifts the artificial constraints imposed by the choice of any local parametrization of the rotation matrices that describe the attitude of the vehicles. Furthermore, the exploitation of the geometry of the state space SE(3) allows for the computation of the first and second derivatives of the vehicle dynamics, cost, and constraints in an intrinsic fashion, thus avoiding the computation of first and second derivatives of the local parametrization, which leads to computational advantages. State and inputs constraints are handled using the barrier function approach [3].

Solving complex motion planning problems for real time applications is a challenging task. We expect that the computational method we are developing will be coupled with other recent planning philosophies such motions primitives [4] or multi-level planners [5] (e.g., to obtain a system trajectory after the graph search phase in a roadmap is completed).

The literature on vehicle motion planning is vast and defies a simple summary. The plethora of methodologies available are quite diverse; we refer to, e.g., [6], [7], [8] and the references therein for a recent account.

The key contributions of this paper are threefold: i) it is shown that the Lie group projection operator approach can be used to solve constrained motion planning problem for multiple vehicles, demonstrating its use on the Lie group SE(3); ii) it is the first time that the barrier function approach (cf. [3]) is applied to solve a constrained optimal control problem on a Lie group. In particular, we detail how to compute first and second order derivatives of $N(N-1)/2$ constraint functions that act pairwise on a set of N vehicles; finally, iii) the paper provides numerical evidence that the Lie group projection operator might be a viable auxiliary tool for investigating sub-Riemannian geometric problems on Lie groups.

Geometric methods are becoming standard tools in numer-

A. Saccon, A.P. Aguiar, A.J. Häusler, and A.M. Pascoal are with LARSyS, IST, Technical University of Lisbon (UTL), Portugal {asaccon, pedro, ahaeusler, antonio}@isr.ist.utl.pt

J. Hauser is with the Department of Electrical, Computer, and Energy Engineering, University of Colorado at Boulder, USA john.hauser@colorado.edu

This work was supported in part by projects CONAV/FCT-PT (PTDC/EEACRO/113820/2009), FCT (PEst-OE/EEI/LA0009/2011), MORPH (EU FP7 under grant agreement No. 288704), and the US AFOSR grant FA9550-09-1-0470. The first author benefited from a postdoctoral scholarship of FCT.

ical integration [9], [10] and optimization [11]. However, not so many numerical methods are available for solving optimal control problems for dynamical systems whose configuration space is a differentiable manifold. Noticeable and interesting exceptions are the discrete-time methods presented in [12], [13], [14], [15] for *mechanical systems* on Lie groups.

This paper is organized as follows. Mathematical preliminaries and a review of the projection operator approach are given in Section II. In Section III, we detail the constrained optimization problem addressed in this paper. In Section IV, we explain how the constrained optimization problem can be addressed via the Lie group projection operator approach. In Section V, we discuss the optimal descent direction subproblem. A sample calculation is presented in Section VI to demonstrate the effectiveness of the method. Conclusions are drawn in Section VII.

II. Preliminaries

We assume that the reader is familiar with the theory of finite dimensional smooth manifolds, covariant differentiation [16], [17], [18], and matrix Lie groups [19], [20].

A. Notations and definitions

M, N	smooth manifolds
TM, T^*M	tangent and cotangent bundles
$f: M \to N$	(smooth) mapping from M to N
$\mathbf{D}f: TM \to TN.$	tangent map of f
$\mathbb{D}^2 f(x) \cdot (\mathrm{v}, \mathrm{w})$	second covariant derivative of f [1]
G	Lie group
$\mathfrak{g}$	Lie algebra of G
e	group identity
$L_g x$, $R_g x$	left and right translations
gx, xg,	shorthand notation for $L_g x$ and $R_g x$
$g\mathrm{v}_x$, $\mathrm{v}_x g$	shorthand notation for $\mathbf{D}L_g(x) \cdot \mathrm{v}_x$ and $\mathbf{D}R_g(x) \cdot \mathrm{v}_x$
$[\cdot, \cdot]$	Lie bracket operation
Ad_g	adjoint representation of G on $\mathfrak{g}$
ad_ϱ	adjoint representation of $\mathfrak{g}$ onto itself ($\mathrm{ad}_\varrho \varsigma = [\varrho, \varsigma]$)
$\exp: \mathfrak{g} \to G$	exponential map
$\log: G \to \mathfrak{g}$	logarithm map (i.e., inverse of $\exp$ in a neighborhood of e)
$\mathrm{SO}(3)$	special orthogonal group
$\mathrm{SE}(3)$	special Euclidean group
$\mathfrak{so}(3)$	Lie algebra of $\mathrm{SO}(3)$
$\mathfrak{se}(3)$	Lie algebra of $\mathrm{SE}(3)$
$\mathbb{R}^3_\times$	Lie algebra on $\mathbb{R}^3$ with cross product as bracket
$\wedge: \mathbb{R}^3_\times \mapsto \mathfrak{so}(3)$	Lie algebra isomorphism $\begin{bmatrix} x_1 \\ x_2 \\ x_3 \end{bmatrix}^\wedge \mapsto \begin{bmatrix} 0 & -x_3 & x_2 \\ x_3 & 0 & -x_1 \\ -x_2 & x_1 & 0 \end{bmatrix}$
$\vee: \mathfrak{so}(3) \mapsto \mathbb{R}^3_\times$	inverse of $\wedge$

B. *The Lie group* $\mathrm{SE}(3)$

In matrix form, every element $(\mathbf{R}, \mathbf{p})$ of $\mathrm{SE}(3)$ is represented as

$$\begin{bmatrix} \mathbf{R} & \mathbf{p} \\ 0 & 1 \end{bmatrix}. \tag{1}$$

An element of the Lie algebra $\mathfrak{se}(3)$ is a matrix

$$\begin{bmatrix} (z^{\mathbf{R}})^\wedge & z^{\mathbf{p}} \\ 0 & 0 \end{bmatrix} \tag{2}$$

with $z^{\mathbf{R}}, z^{\mathbf{p}} \in \mathbb{R}^3$. As a vector, we can represent is as $z = (z^{\mathbf{R}}, z^{\mathbf{p}}) \in \mathbb{R}^6$. This corresponds to a choice of an ordered basis for $\mathfrak{se}(3)$. Given this choice of a basis, the adjoint map ad_z is simply given by the 6×6 real matrix (recall that $\mathrm{ad}_{z_1} z_2 = [z_1, z_2]$)

$$\mathrm{ad}_z = \begin{bmatrix} (z^{\mathbf{R}})^\wedge & 0 \\ (z^{\mathbf{p}})^\wedge & (z^{\mathbf{R}})^\wedge \end{bmatrix}. \tag{3}$$

The exponential and logarithm maps of $\mathrm{SE}(3)$ can be computed as reported in, e.g., [21].

C. *The Lie group projection operator approach*

The projection operator approach [22], [1], is a direct method for solving continuous time optimal control problems generating a sequence of trajectories with decreasing cost. It differs from classical methods as it does not rely on a transcription phase where the system dynamics and cost functional are discretized in order to obtain a nonlinear optimization problem. Rather, a quadratic approximation of the optimal control problem is directly constructed in continuous time. Each iteration of the algorithm amounts to integrating the vehicle dynamics and solving an associated Riccati equations by means of an ordinary differential equation solver. Implementations details and numerical experiments on $\mathrm{SO}(3)$ and $T\mathrm{SO}(3)$ have been presented in [2], [23].

In [1], the authors have shown how the approach presented in [22] can be generalized to work with a dynamical system defined on a Lie group G, that is, for a system in the form

$$\dot{g} = f(g, u, t) = g(t)\lambda(g(t), u(t), t)\,, \tag{4}$$

where $f: G \times \mathbb{R}^m \times \mathbb{R} \to TG$ is a control system on G and $\lambda: G \times \mathbb{R}^m \times \mathbb{R} \to \mathfrak{g}$, $\lambda(g, u, t) := g^{-1} f(g, u, t)$, is its *left-trivialization*. The approach, in its simplest formulation, can handle optimal control problems in the form

$$\min_{(g,u)(\cdot)} \int_0^T l(g(\tau), u(\tau), \tau)\, d\tau + m(g(T)) \tag{5}$$

subject to

$$\dot{g} = f(g, u, t), \tag{6}$$

$$g(0) = g_0, \tag{7}$$

where $l: G \times \mathbb{R}^m \times \mathbb{R} \to \mathbb{R}$ is the incremental cost, $m: G \to \mathbb{R}$ the terminal cost, and g_0 the initial condition. Modifications of the strategy for handling a terminal condition and mixed input-state constraints (through a barrier functional approach) are discussed, for control problems on $\mathbb{R}^n$, in [24] and [3].

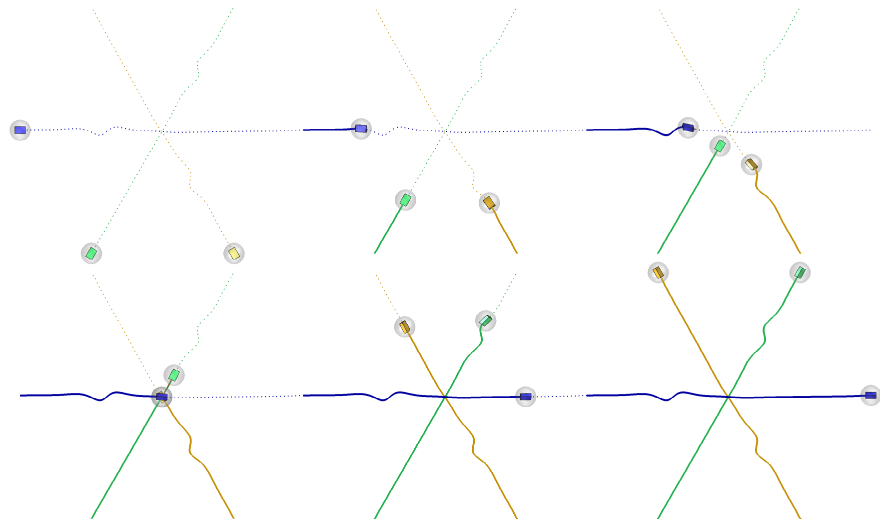

Fig. 1. Snapshots of the planned vehicle trajectories (seen from above). The plot corresponds to the time instants $[0.00, 2.00, 4.00, 5.34, 8.00, 10.00]$.

Roughly speaking, the projection operator approach can be thought as a Newton method in infinite dimension. The approach is based on (and derives its name from) the projection operator $\mathcal{P}$ [25], which is an operator that maps a generic curve $\xi(t) = (\alpha(t), \mu(t)) \in G \times \mathbb{R}^m$, $t > 0$, into a trajectory $\eta(t) = (g(t), u(t)) \in G \times \mathbb{R}^m$, $t > 0$, of the system (4). The operator $\mathcal{P}$ is defined through the feedback system

$$\begin{aligned} \dot g(t) &= g(t)\lambda(g(t), u(t), t)\,, \quad g(0) = \alpha(0)\,, \\ u(t) &= \mu(t) + K(t)\big[\log(g(t)^{-1}\alpha(t))\big]\,, \end{aligned} \tag{8}$$

where $K(t) : \mathfrak{g} \to \mathbb{R}^m$ is a linear map, which can be thought as a standard linear feedback as soon as a basis is chosen for the Lie algebra $\mathfrak{g}$. It is straightforward to verify that $\mathcal{P}$ is indeed a projection, i.e., it satisfies $\mathcal{P}^2 := \mathcal{P} \circ \mathcal{P} = \mathcal{P}$.

Given a *trajectory* $\xi(t) = (g(t), u(t))$ of the control system (4), its (left-trivialized) linearization is defined as the time-varying linear system

$$\dot z(t) = A(\xi(t), t) z(t) + B(\xi(t), t) v(t), \tag{9}$$

with $(z(t), v(t)) \in \mathfrak{g} \times \mathbb{R}^m$, $t \geq 0$ and where

$$A(\xi, t) := \mathbf{D}_1 \lambda(g, u, t) \circ T_e L_g - \mathrm{ad}_{\lambda(g,u,t)}, \tag{10}$$

$$B(\xi, t) := \mathbf{D}_2 \lambda(g, u, t). \tag{11}$$

The projection operator approach consists in applying the following iterative method

Algorithm (Projection operator Newton method)
given initial trajectory $\xi_0 \in \mathcal{T}$
for $i = 0, 1, 2, \ldots$

(search direction)

$$\zeta_i = \arg \min_{\xi_i \zeta \in T_{\xi_i} \mathcal{T}} \mathbf{D}h(\xi_i) \cdot \xi_i \zeta + \tfrac{1}{2} \mathbb{D}^2 \tilde h(\xi_i) \cdot (\xi_i \zeta, \xi_i \zeta) \tag{12}$$

$$\gamma_i = \arg \min_{\gamma \in (0,1]} \tilde h(\xi_i \exp(\gamma \zeta_i)) \qquad \text{(step size)} \tag{13}$$

$$\xi_{i+1} = \mathcal{P}(\xi_i \exp(\gamma_i \zeta_i)) \qquad \text{(update)} \tag{14}$$

end

In (12), h is the cost functional appearing in (5) and $\tilde h$ is the functional obtained by composing h with the projection operator $\mathcal{P}$, i.e., $\tilde h := h \circ \mathcal{P}$. At each iterate, the search direction minimization (12) is performed on the tangent space $T_\xi \mathcal{T}$, that is, we search over the curves $\zeta(\cdot) = (z(\cdot), v(\cdot))$ that satisfies (9). Then, the step size subproblem (13) is considered. The classical *approximate* solution obtained using backtracking line search with Armijo condition [26, Chapter 3] can be used to compute the optimal step size γ_i. Finally, the update step (14) *projects* each iterate on to the trajectory manifold and the process restarts as long as termination conditions have not been met.

The convergence to a local minimum that satisfies second order sufficient conditions for optimality can be readily checked.

III. The Optimal Motion Planning Problem

The motion planning problem that we consider can be briefly described as follows. Given a fixed time interval $[0, T]$, $T > 0$, and a number of vehicles N, compute the inputs that steer them from a given initial pose at at time $t = 0$ to a desired final one at time $t = T$ while minimizing an energy-related criterion and avoiding inter-vehicle collisions.

A. Vehicle dynamics

In what follows, the state of the i-th vehicle is represented by an element of the Lie group SE(3) as $\mathbf{g}^{[i]} = (\mathbf{R}^{[i]}, \mathbf{p}^{[i]})$, $i \in \{1, 2, \ldots, N\}$. At the kinematic level, the motion of each vehicle is described by the equations

$$\dot{\mathbf{R}}^{[i]} = \mathbf{R}^{[i]}\big(0; q^{[i]}; r^{[i]}\big)^\wedge, \tag{15}$$

$$\dot{\mathbf{p}}^{[i]} = \mathbf{R}^{[i]}\big(u^{[i]}; 0; 0\big), \tag{16}$$

where ; denotes row concatenation. In the above equations, the inputs for the i-th kinematic model are the pitch rate

$q^{[i]}$, yaw rate $r^{[i]}$, and longitudinal velocity $u^{[i]}$. It is possible to show that the *driftless* left-invariant control-affine system (15)-(16) is controllable as it satisfies the Lie algebra rank condition (LARC).

In compact form, we write the input of the i-th vehicle as $\mathbf{u}^{[i]}(t) = (q^{[i]}(t); r^{[i]}(t); u^{[i]}(t)) \in \mathbb{R}^3$ and the dynamics (15)-(16) as

$$\dot{\mathbf{g}}^{[i]}(t) = f^{[i]}\big(\mathbf{g}^{[i]}(t), \mathbf{u}^{[i]}(t)\big). \tag{17}$$

B. *The motion planning problem*

The motion planning is obtained by solving the optimal control problem

$$\min_{(\mathbf{g},\mathbf{u})(\cdot)} \int_0^T \frac{1}{2}\sum_{i=1}^{N} \big\|\mathbf{u}^{[i]}(\tau)\big\|_R^2 d\tau, \tag{18}$$

where $\mathbb{R}^{3\times 3} \ni R = R^T > 0$ is a weighting matrix, subject to the dynamic constraint

$$\dot{\mathbf{g}}(t) = f\big(\mathbf{g}(t), \mathbf{u}(t)\big), \tag{19}$$

with initial and final constraints

$$\mathbf{R}^{[i]}(0) = \mathbf{R}_0^{[i]}, \qquad \mathbf{R}^{[i]}(T) = \mathbf{R}_f^{[i]}, \tag{20}$$

$$\mathbf{p}^{[i]}(0) = \mathbf{p}_0^{[i]}, \qquad \mathbf{p}^{[i]}(T) = \mathbf{p}_f^{[i]}, \tag{21}$$

for $i \in 1, \ldots, N$. The *collective* dynamics (19) is obtained by stacking all the control systems (17) into a control system with state $\mathbf{g} = (\mathbf{g}^{[1]}, \mathbf{g}^{[2]}, \ldots, \mathbf{g}^{[N]}) \in \mathrm{SE}(3)^N$ and input $\mathbf{u} = (\mathbf{u}^{[1]}, \mathbf{u}^{[2]}, \ldots, \mathbf{u}^{[N]}) \in \mathbb{R}^{3N}$. Note that in this paper the product Lie group $\mathrm{SE}(3)^N$ will play the role of the Lie group G discussed in Section II. We furthermore impose $N_c = N(N-1)/2$ collision constraints

$$\|\mathbf{p}^{[i]}(t) - \mathbf{p}^{[j]}(t)\|^2/D^2 - 1 \geq 0 \tag{22}$$

for $i, j \in \{1, \ldots, N\}$, $i < j$, and $t \in [0, T]$. The collision constraint (22) requires that the distance between any two vehicles is never less than a fixed distance D. To visualize this set of constraints, one may imagine that each vehicle is contained within a safety spherical hull of diameter D and that, during a manuever, the spheres are to remain essentially intersection free, being allowed to just touch one another.

IV. Solving the Motion Planning Problem

We handle the inequality constraints on the state and control through the barrier function approach described in [3]. The terminal constraint is indirectly (and approximately) addressed using a terminal cost penalty, cf. [24]. Therefore, given the optimal motion planning problem introduced in Section III-B, from the cost functional (18) and inequality constraints (22), we obtain the augmented cost functional

$$\int_0^T l(\mathbf{g}, \mathbf{u}) + \sum_{k=1}^{N_c} \varepsilon \beta_\delta(c_k(\mathbf{g}, \mathbf{u}))\, d\tau + m(\mathbf{g}(T)) \tag{23}$$

where

$$l(\mathbf{g}, \mathbf{u}) := \frac{1}{2}\sum_{i=1}^{N} \big\|\mathbf{u}^{[i]}\big\|_R^2, \tag{24}$$

$$c_k(\mathbf{g}, \mathbf{u}) := \big\|\mathbf{p}^{[i]} - \mathbf{p}^{[j]}\big\|^2/D^2 - 1 \tag{25}$$

with $i,j \in \{1, \ldots, N\}$, $i < j$, and $k = k(i,j) \in \{1, ..., N_c\}$. The terminal cost is defined as

$$m_\rho(\mathbf{g}) := \frac{1}{2}\sum_{i=1}^{N} \rho_{\mathbf{R}} \big\|I - \big(\mathbf{R}_f^{[i]}\big)^T \mathbf{R}^{[i]}\big\|^2 + \rho_{\mathbf{p}} \big\|\mathbf{p}^{[i]} - \mathbf{p}_f^{[i]}\big\|^2, \tag{26}$$

with $\rho = (\rho_{\mathbf{R}}, \rho_{\mathbf{p}})$. We now explain in details the cost (23).

a) Constraint indexing: Each collision constraint is indexed through the index k. This index is computed from the indexes i and j of the two vehicles to which the constraint applies. For a generic value of N, one gets $k(i,j) = j + i(N-1) - i(i+1)/2$, $i < j$, i, $j \in \{1, \ldots, N\}$. For $N = 3$, e.g., $k(1,2) = 1$, $k(1,3) = 2$, and $k(2,3) = 3$. For reasons that will be clarified later, we define $k(j,i) = k(i,j)$, $i \leq j$, and $k(i,i) = 0$, $i \in \{1, \ldots, N\}$, making $[k(i,j)]$ into a symmetric matrix.

b) Modified barrier function: In this work, we use an approximate barrier function based on the one proposed in [3] that is well adapted to constraints of the form (22). Recall that [3], for $0 < \delta \leq 1$,

$$\tilde{\beta}_\delta(z) = \begin{cases} -\log z & z > \delta \\ \dfrac{k-1}{k}\left[\left(\dfrac{z - k\delta}{(k-1)\delta}\right)^k - 1\right] - \log\delta & z \leq \delta \end{cases}$$

provides an approximate log barrier function that can be evaluated outside of the strictly feasible region $z > 0$. (Here $k > 1$ is an even integer, usually taken to be $k = 2$.) In many applications, including those using an input constraint like $1 - \|u\|^2 \geq 0$, the constraint function is naturally bounded above by 1. On the other hand, an exclusion constraint function such as $c_k(\mathbf{g}, \mathbf{u})$ in (25) will often have values substantially greater than 1, resulting in an (artificially) lower than expected cost in (23) due to the possibly large magnitude of $-\log c_k(\mathbf{g}, \mathbf{u})(\tau)$. To capture the fact that we only want to penalize attempted collisions, we make use of the "hockey stick" function

$$\sigma(z) = \begin{cases} \tanh(z) & z \geq 0 \\ z & \text{otherwise} \end{cases} \tag{27}$$

to saturate each exclusion constraint function $c_k(\mathbf{g}, \mathbf{u})$ expressing, in exponential fashion (look at $-\log\tanh z$, $z > 0$), the manner in which our concern for collision fades as the separation distance increases. The approximate barrier function in (23) will thus be taken to be $\beta_\delta(z) = \tilde{\beta}_\delta(\sigma(z))$.

c) Terminal cost m: The terminal cost (26) weighs the deviation of the final state $\mathbf{g}^{[i]}(T) = (\mathbf{R}^{[i]}(T), \mathbf{p}^{[i]}(T))$ from the desired final state $\mathbf{g}_f^{[i]} = (\mathbf{R}_f^{[i]}, \mathbf{p}_f^{[i]})$. Note that $\|I - \mathbf{R}\|^2$ refers to the squared Frobenius norm $\mathrm{tr}((I - \mathbf{R})^T(I - \mathbf{R}))$ that, together with its first and second (covariant) derivatives, has been described in [2], [23]. The parameters $\rho_{\mathbf{R}}$ and $\rho_{\mathbf{p}}$ are chosen large enough to ensure that the final state of each vehicle approaches the desired terminal condition with a prescribed tolerance (penalty approach).

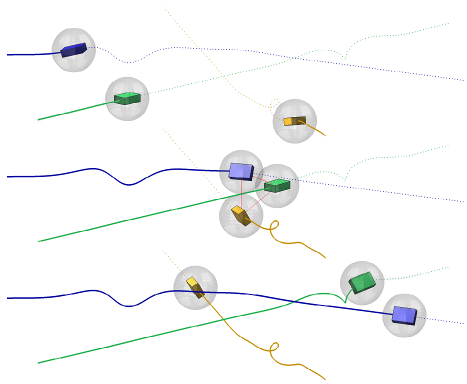

Fig. 2. Detailed snapshots of the vehicle trajectories in proximity of a possible collision. The plot corresponds to the time instants $[4.00, 5.34, 8.00]$.

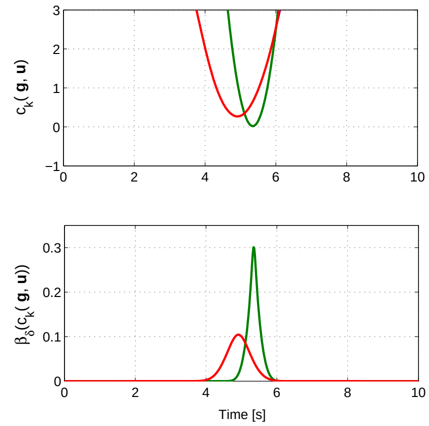

Fig. 3. Constraint function, without and with the evaluation of barrier function β_δ, respectively. In the bottom plot, $\delta = 10^{-8}$.

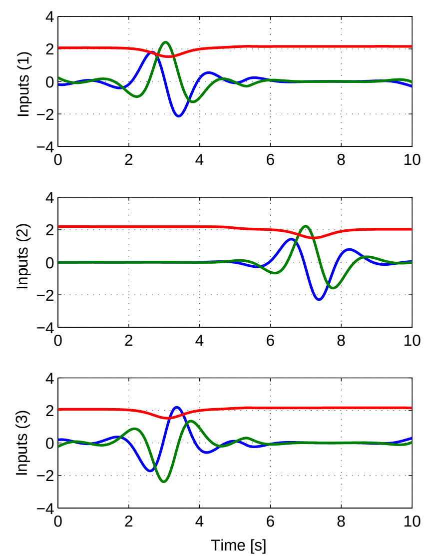

Fig. 4. Control inputs for the 3 vehicles. Respectively, the blue (1), green (2), and yellow (3) vehicle. Pitch rate (q) is blue, yaw rate (r) is green, and longitudinal speed (u) is red.

V. Optimal Descent Direction

The descent direction for the projection operator Newton method is computed by solving the subproblem (12). As shown in [2], given a trajectory $\xi(t) = (\mathbf{g}(t), \mathbf{u}(t))$ of (19), $t \in [0, T]$, the subproblem (12) is equivalent to solving a LQ optimal control problem of the form

$$\min_{(z,v)(\cdot)} \int_0^T a(\tau)^T z(\tau) + b(\tau)^T v(\tau) + \frac{1}{2} \begin{bmatrix} z(\tau) \\ v(\tau) \end{bmatrix}^T W(\tau) \begin{bmatrix} z(\tau) \\ v(\tau) \end{bmatrix} d\tau + a_1^T z(T) + \frac{1}{2} z(T)^T P_1 z(T) , \tag{28}$$

subject to the dynamic constraint

$$\dot{z}(t) = A(\xi(t)) z(t) + B(\xi(t)) v(t) , \tag{29}$$
$$z(0) = 0 . \tag{30}$$

The general expressions for the left-trivialized linearization A and B appearing in (29) has been given in (10) and (11), respectively. The general expressions of the vectors a, b, a_1 and matrices W, P_1 in terms of the (left-trivialized) dynamics λ and the integral cost l, and terminal cost m are given in [2]. Due to space limitations, we will not provide the expressions of these quantities. An extended, eight pages version of this paper containing the explicit expressions for the special case of the cost (23) and dynamics (19) is readily available upon direct request to the authors.

VI. Sample Calculation

We consider in this section a planning example for three vehicles. The example shows the effectiveness of the planner in finding trajectories for the three vehicles that match the prescribed initial and final conditions and avoid inter-vehicle collisions. The scenario is depicted in Figure 1. The planned trajectory has a total duration of 10 seconds and 6 snapshots of the animation are shown.

The desired initial and final vehicle positions lie at the corners of an hexagon and each vehicle must reach the corner opposite to the one it starts from. The hexagon diameter has length 20 m. Starting with a zero initial roll angle, each vehicle must reach the final position with a roll angle of 60 degrees.

Because no direct control of the roll velocity is available, the planner generates the desired roll motion mainly by cycling the yaw and pitch rate commands, exploiting the nonlinear controllability of the model. This phenomenon is evident by looking at the optimal inputs given in Figure 4. Its effect on the roll angle of each vehicle can be appreciated in Figure 1, where one can also see the cycling motion in the yaw angle. Two vehicles (blue and yellow) perform this wiggling at the beginning of the optimal maneuver, while the third (green) waits until it “slips through” the other two vehicles, thus avoiding a possible collision. The speed of each vehicle is kept approximately equal to 2 m/s as each vehicle has to cover a distance of approximately 20 m in 10 s.

The collision between the two slower vehicles does not occur as one passes on top of the other as shown in the detailed snapshots of Figure 2. We can monitor at each iteration the value of the constraint functions by plotting the value of $c_k(\mathbf{g}(t), \mathbf{u}(t))$, $t \in [0,T]$, $k \in \{1,2,3\}$ as shown in the upper part of Figure 3. Due to the symmetry of the problem, two constraints take the same value along the optimal trajectory (the distance of the green-yellow and the green-blue vehicle pairs is the same). The touching of the spherical hulls of the yellow and blue vehicles is reflected in the fact that the corresponding constraint function goes to zero. The graph at the bottom of Figure 3 makes evident the role of the barrier function β_δ in penalizing the possible collision between the hulls. Note how $\beta_\delta(c_k(\mathbf{g}, \mathbf{u}))$ gets larger as the corresponding constraint function $c_k(\mathbf{g}, \mathbf{u})$ approaches zero.

VII. CONCLUSIONS

We have discussed the application of the Lie group projection operator approach to a constrained optimization problem involving a set of dynamics systems on $\mathrm{SE}(3)$. We have detailed how to construct the quadratic approximation of the original problem and, in particular, how to compute the first and second derivative of the constraint functions that arise in the problem of cooperative planning for a group of N vehicles. A sample computation was discussed, showing that with this approach it is possible to compute a optimal trajectory that solves the constrained optimization problem, improving the confidence that the strategy can be a viable way to deal with more complex vehicle dynamics and geometric constraints. Convergence rate, existence and uniqueness, executions time, updating rules for the constraint parameters ε and δ, and further implementation issues will be addressed in future work.

For a single vehicle (and no collision constraints), the particular optimal control problem studied in this paper corresponds to the computation of the geodesics for a sub-Riemannian manifold defined on the Lie groups $\mathrm{SE}(3)$ [27], [28], [29], [30]. The Lie group projection operator approach might be therefore used as an auxiliary tool in the study of this interesting branch of differential geometry. Further research is required however to understand if, e.g., we can obtain strictly abnormal minimizers [31].

REFERENCES

[1] A. Saccon, J. Hauser, and A. P. Aguiar, "Optimal Control on Non-Compact Lie Groups: A Projection Operator Approach," in *49th IEEE Conference on Decision and Control (CDC)*. IEEE, 2010, pp. 7111–7116.

[2] A. Saccon, J. Hauser, and A. Aguiar, "Optimal Control on Lie Groups: Implementation Details of the Projection Operator Approach," in *IFAC world congress*, 2011, pp. 14 567–14 572.

[3] J. Hauser and A. Saccon, "A Barrier Function Method for the Optimization of Trajectory Functionals with Constraints," in *Proceedings of the 45th IEEE Conference on Decision and Control*. IEEE, 2006, pp. 864–869.

[4] E. Frazzoli, M. A. Dahleh, and E. Feron, "Maneuver-Based Motion Planning for Nonlinear Systems With Symmetries," *Robotics, IEEE Transactions on*, vol. 21, no. 6, pp. 1077–1091, 2005.

[5] C. Goerzen, Z. Kong, and B. Mettler, "A Survey of Motion Planning Algorithms from the Perspective of Autonomous UAV Guidance," *Journal of Intelligent and Robotic Systems*, vol. 57, no. 1-4, pp. 65–100, 2010.

[6] S. M. LaValle, *Planning Algorithms*. Cambridge, UK: Cambridge University Press, 2006.

[7] B. Siciliano and O. Khatib, *Springer Handbook of Robotics*. Springer, 2008.

[8] F. Fahimi, *Autonomous Robots Modeling, Path Planning, and Control*. Springer, Canada, 2009.

[9] A. Iserles, H. Z. Munthe-Kaas, S. P. Nörsett, and A. Zanna, "Lie-group methods," *Acta numerica*, vol. 9, pp. 215–365, 2001.

[10] E. Hairer, C. Lubich, and G. Wanner, *Geometric Numerical Integration*, 2nd ed. Springer-Verlag Berlin Heidelberg, 2006.

[11] P.-A. Absil, R. Mahony, and R. Sepulchre, *Optimization Algorithm on Matrix Manifolds*. Princeton University Press, 2008.

[12] O. Junge, J. E. Marsden, and S. Ober-Blöbaum, "Discrete mechanics and optimal control," in *16th IFAC World Congress*, 2005.

[13] M. Kobilarov, M. Desbrun, J. E. Marsden, and G. S. Sukhatme, "A discrete geometric optimal control framework for systems with symmetries," in *Proceedings of Robotics: Science and Systems*, vol. 3, Atlanta, GA, USA, 2007.

[14] T. Lee, M. Leok, and N. H. Mc˜Clamroch, "Optimal Attitude Control of a Rigid Body using geometrically exact computations on $\{\mathrm{SO}\}(3)$," *Journal of Dynamical and Control Systems*, vol. 14, no. 4, pp. 465–487, 2008.

[15] M. B. Kobilarov and J. E. Marsden, "Discrete Geometric Optimal Control on Lie Groups," *IEEE Transactions on Robotics*, vol. 27, no. 4, pp. 641–655, Aug. 2011.

[16] W. M. Boothby, *An Introduction to Differentiable Manifolds and Riemannian Geometry*, 2nd ed., ser. Pure and applied mathematics. Academic Press, Boston, 1986.

[17] R. Abraham, J. E. Marsden, and T. Ratiu, *Manifolds, tensor analysis, and applications*. Springer-Verlag, New York, 1988.

[18] J. M. Lee, *Riemannian manifolds: an introduction to curvature*. Springer, New York, 1997.

[19] V. S. Varadarajan, *Lie Groups, Lie Algebras, and Their Representations*. Springer-Verlag, New York, 1984.

[20] W. Rossmann, *Lie Groups. an Introduction through Linear Groups*. Oxford University Press, 2002.

[21] F. Bullo and R. M. Murray, "Proportional Derivative (PD) Control on the Euclidean Group," California Institute of Technology, Pasadena, CA, USA, Tech. Rep.

[22] J. Hauser, "A Projection Operator Approach to the Optimization of Trajectory Functionals," in *Proceedings of the 15th IFAC World Congress*, Barcelona, Spain, 2002.

[23] A. Saccon, A. P. Aguiar, and J. Hauser, "Lie Group Projection Operator Approach : Optimal Control on T SO (3)," in *Proceedings of the 50th IEEE Conference on Decision and Control and European Control Conference (CDC-ECC)*, Orlando, FL, USA, 2011, pp. 6973 – 6978.

[24] J. Hauser, "On the Computation of Optimal State Transfers with application to the Control of Quantum Spin Systems," in *American Control Conference (ACC)*, 2003.

[25] ——, "A Projection Operator Approach to the Optimization of Trajectory Functionals," in *15th IFAC World Congress*, Barcelona, Spain, 2002.

[26] J. Nocedal and S. J. Wright, *Numerical optimization*, 2nd ed. Springer Science+Business Media LLC., 2006.

[27] R. Brockett, "Control theory and singular Riemannian geometry," in *New directions in Applied Mathematics*, P. J. Hilton and G. S. Young, Eds. Springer, New York, 1981, pp. 11–27.

[28] R. S. Strichartz, "Sub-riemannian geometry," *J. Differential Geom*, vol. 24, no. 2, pp. 221–263, 1986.

[29] ——, "Corrections to "Sub-Riemanannian Geometry"," *Journal of Differential Geometry*, vol. 30, pp. 595–596, 1989.

[30] R. Montgomery, "A survey of singular curves in sub-Riemannian geometry," *Journal of Dynamical and Control Systems*, vol. 1, no. 1, pp. 49–90, 1995.

[31] H. Sussmann, "A cornucopia of four-dimensional abnormal subriemannian minimizers," in *Sub-Riemannian geometry*, A. Bellaïche and J.-J. Risler, Eds. Basel: Birkhäuser, 1996, pp. 341–364.